Molecular mechanism of recombinant liver fatty acid binding protein's antioxidant activity

Jing Yan,* Yuewen Gong,*,† Yi-Min She,§ Guqi Wang, Michael S. Roberts,†† and Frank J. Burczynski[1],*,§§**

Faculty of Pharmacy,* Section of Hepatology,† Department of Internal Medicine, Department of Pharmacology and Therapeutics, and Faculty of Medicine,§§ University of Manitoba, Winnipeg, Canada; Centre for Biologics Research,§ Biologics and Genetic Therapies Directorate, Health Canada, Ottawa, Ontario K1A 0K9, Canada; McColl-Lockwood Laboratory,** Cannon Research Center, Charlotte, NC 28232-2861; and Department of Medicine,†† Princess Alexandra Hospital, University of Queensland, Woolloongabba, Queensland, Australia 4102

Abstract Hepatocytes expressing liver fatty acid binding protein (L-FABP) are known to be more resistant to oxidative stress than those devoid of this protein. The mechanism for the observed antioxidant activity is not known. We examined the antioxidant mechanism of a recombinant rat L-FABP in the presence of a hydrophilic (AAPH) or lipophilic (AMVN) free radical generator. Recombinant L-FABP amino acid sequence and its amino acid oxidative products following oxidation were identified by MALDI quadrupole time-of-flight MS after being digested by endoproteinase Glu-C. L-FABP was observed to have better antioxidative activity when free radicals were generated by the hydrophilic generator than by the lipophilic generator. Oxidative modification of L-FABP included up to five methionine oxidative peptide products with a total of ~80 Da mass shift compared with native L-FABP. Protection against lipid peroxidation of L-FABP after binding with palmitate or α-bromo-palmitate by the AAPH or AMVN free radical generators indicated that ligand binding can partially block antioxidant activity. We conclude that the mechanism of L-FABP's antioxidant activity is through inactivation of the free radicals by L-FABP's methionine and cysteine amino acids. Moreover, exposure of the L-FABP binding site further promotes its antioxidant activity. In this manner, L-FABP serves as a hepatocellular antioxidant.—Yan, J., Y. Gong, Y-M. She, G. Wang, M. S. Roberts, F. J. Burczynski. **Molecular mechanism of recombinant liver fatty acid binding protein's antioxidant activity.** ***J. Lipid Res.*** **2009.** 50: **2445–2454.**

Supplementary key words hepatocyte • oxidative stress • free radical

Liver fatty acid binding protein (L-FABP) is a low molecular weight protein (14–15 kDa) that belongs to a family of lipid binding proteins (1). The protein was first discovered by Ockner et al. in 1972 (2) and was originally named Z-protein. Since that time, there has been an explosive growth in information regarding the role of L-FABP in cellular homeostasis. While FABPs are present in many tissues, such as heart, brain, intestinal, skin, adipose, muscle, epidermal, ileal, myelin, and testis, L-FABP is found in abundance in hepatocytes where it accounts for ~2% of the total cellular protein. Although L-FABP is abundant in the liver, it also is present in tissues such as murine alveolar macrophages (3), kidney (4), and intestine (5).

L-FABP is made up of 127 amino acids that compose 10 antiparallel β-strands. These stands are organized into two five-stranded β-sheets and two α-helices. The two α-helices are hypothesized to function as a portal that controls entry and release of ligands from the binding pocket created by the β-strands (6). A large interior water-filled cavity forms the confines of the β-strands, which serve as the hydrophobic ligand-binding site. L-FABP is able to bind and translocate many lipophilic substrates throughout the cytosol. Some of these substrates include long-chain fatty acids (7–9), bile acids (10), eicosanoids (11), and hypolipidemic drugs (12). Transfer of these ligands from L-FABP to membranes is thought to occur by a diffusive process; i.e., the ligand first dissociates from the binding pocket and then diffuses to its site of action, while transfer of ligands from other FABPs, such as I-FABP, is thought to occur by a direct collisional interaction (13). It seems that L-FABP also plays a role in transferring bound ligands into the nucleus. These ligands could activate the peroxisome proliferator-activated receptor α nuclear receptors and

This work was supported by an operating grant from the Canadian Institute of Health Research.

Manuscript received 14 April 2009 and in revised form 26 May 2009.

Published, JLR Papers in Press, May 27, 2009
DOI 10.1194/jlr.M900177-JLR200

Abbreviations: DCF, dichlorofluorescein; DCFH-DA, 2′,7′-dichlorofluorescin-diacetate; GST, glutathione *S*-transferase; L-FABP, liver fatty acid binding protein; ROS, reactive oxygen species; TBARS, thiobarbituric acid-reactive substance.

[1]To whom correspondence should be addressed.
e-mail: burczyn@cc.umanitoba.ca

thus initiate transcriptional activity that could affect lipid and glucose metabolism among other effects (14–18).

A unique property of L-FABP that has escaped detection is its antioxidant effect. L-FABP is known to bind polyunsaturated fatty acids (19) and long-chain fatty acid peroxidation products (11). By binding polyunsaturated fatty acids, L-FABP modulates the availability of these fatty acids to intracellular oxidative pathways (19) and in this manner controls the amount of reactive oxygen species (ROS) released within the cell from this pathway. In addition to these well-known functions, recent studies have shown that L-FABP plays a further role in the cellular antioxidant defense mechanism (20–22). Using an L-FABP cDNA transfection model Wang et al. (20) reported that hepatocytes containing L-FABP were associated with much lower levels of ROS compared with hepatocytes devoid of L-FABP. Using a bile-duct ligated model of cholestasis, this group further showed that clofibrate increased L-FABP levels were associated with improved hepatic function and reduced lipid peroxidation products (21). The antioxidative function of L-FABP is thought to be due to its amino acid composition. L-FABP contains one cysteine and several methionine groups that are known to take part in cellular redox cycling. Thus, although the actual mechanism for the L-FABP antioxidant property is not known, it is likely to involve these amino acids. Also unknown is whether L-FABP preferentially inactivates ROS released in lipophilic environments, such as membranes, or in the hydrophilic cytosolic environment. In this study, we investigated the mechanism and efficiency of the recombinant L-FABP antioxidant property when free radicals were released into the aqueous or lipid environments.

MATERIALS AND METHODS

Materials

Plasmid pGEX-6P-2 was purchased from GE Healthcare Bio-Sciences (Baie d'Urfé, Québec, Canada). Restriction enzymes, DNA polymerase, and T4 DNA ligase were obtained from Roche (Laval, Quebec, Canada). The 2,2′-azobis(2,4-dimethylvaleronitrile) and 2,2′-azobis(2-amidinopropane) dihydrochloride were purchased from Wako (Osaka, Japan). All other chemicals were obtained from Sigma Chemical (Oakville, ON, Canada).

Construction, expression, and purification of pGEX-6P-2 with L-FABP

The expression vector pGEX-6P-2 was digested with *Bam*HI and *Xho*I for the insertion of a full-length rat L-FABP cDNA, which was cloned by a pair of gene-specific PCR primers designed by the Oligo 5.1 computer software according to the GenBank sequence (BC086947). The primers contained *Bam*HI and *Xho*I, respectively, and were synthesized by Invitrogen. PCR cloning of rat L-FABP was performed according to our previous publication (20). The plasmid pGEX-6P-2 with L-FABP was constructed according to the pGEX-6P-2 instruction manual, and successful ligation of L-FABP with pGEX-6P-2 was confirmed by restriction enzyme digestion and DNA sequencing.

Rat L-FABP was expressed by transformation into bacteria DH5α and amplified by addition of 0.1 nM isopropyl-β-D-thiogalactoside according to standard protocol. After expression in DH5α, L-FABP was purified according to the manual of pGEX-6p-2. The fusion protein GST/L-FABP was first associated with the glutathione-Sepharose 4B beads, and then the GST/L-FABP was eluted by addition of elution buffer or L-FABP digested from GST by addition of 10 units PreScission Protease and cleavage buffer. Both GST/L-FABP and L-FABP were analyzed by SDS-PAGE and MALDI-quadrupole time-of-flight (QqTOF) MS, respectively.

Characterization of the recombinant protein

SDS-PAGE and Western blot analysis. The resolved proteins were either stained with Coomassie blue for SDS-PAGE or transferred to Nitroplus-2000 membranes for Western immunoblotting as previously outlined by our group (23). For the Western blot, a 15% SDS-polyacrylamide gel was used. Once proteins were separated, bands were transferred onto Nitroplus-2000 membrane (Micron Separations, Westborough, MA). Nonspecific antibody binding was blocked by preincubation of membranes in 1× TBS containing 5% skim milk for 1 h at room temperature. Membranes were then incubated overnight at 4°C with a polyclonal antibody raised against rat L-FABP as described previously (22) in 1× TBS containing 5% skim milk. After being washed, membranes were incubated with donkey anti-rabbit IgG (Amersham) at 1:500 dilution for 1 h (room temperature). Bands were visualized using an enhanced chemiluminescence kit (ECL system; GE Healthcare Bio-Sciences.

MALDI-QqTOF MS. L-FABP proteins (~5 ug) were digested with 50 ng sequencing grade trypsin or endoprotease Glu-C (Roche Diagnostic) in 25 mM ammonium bicarbonate and the solution incubated at 37°C for 6 h. Analyses of the proteolytic peptides were performed on Applied Biosystems/MDS Sciex QStar XL QqTOF mass spectrometer by MALDI at positive ionization mode. The instrument was equipped with a MALDI II source and a UV nitrogen laser operating at 337 nm. Samples were prepared at the ratio of 1:1 (v/v) of the peptide digest to matrix (i.e., 2,5-dihydroxybenzoic acid) in 50% acetonitrile/water and subsequently dried on a stainless steel MALDI plate at room temperature. After MALDI MS mapping, the individual peptide sequences were identified by MS/MS measurements using argon as the collision gas. The intact mass of L-FABP was determined by MALDI and also confirmed by nanospray ESI TOF mass spectrometry using the same instrument. In the case of ESI, the protein sample was dissolved in 50% methanol/0.1% formic acid solution.

Peptide fingerprinting masses were searched by MS-Fit program against the National Center for Biotechnology Information database using ProteinProspector at the UCSF web site (http://prospector.ucsf.edu), whereas the MS/MS ions search on each tandem mass spectrum was performed through the Mascot search engine (MatrixScience; http://www.matrixscience.com). These searches take account of up to three missed enzyme cleavage sites and the modifications of methionine oxidation, asparagine and glutamine deamidation to aspartic acid and glutamic acid, and N-terminal pyroglutamation. Mass tolerance between calculated and observed masses used for database search was considered at the range of ±100 ppm for MS peaks and ±0.2 Da for MS/MS fragment ions. If no result was retrieved by the automated database search, then manual data interpretation was conducted on the spectrum based on the L-FABP predicted sequence.

In vitro dichlorofluorescein fluorescence measurement

As described previously, 2′,7′-dichlorofluorescin-diacetate (DCFH-DA) was used for determining free radical levels released by H_2O_2. Briefly, DCFH-DA was deesterified to generate the oxidation substrate DCFH by mixing 125 μl of a 1.5 mM DCFH-DA

solution in ethanol with 0.5 ml of 0.01 N NaOH for 30 min at room temperature in the dark. The mixture was neutralized with 2.5 ml of 20 mM sodium phosphate buffer (pH 7.0) to give a final concentration of 60 μM of the activated DCFH dye stock solution. The deesterified DCFH-DA could then be oxidized by free radicals to a highly fluorescent dichlorofluorescein (DCF) whose absorbance could be quantitated at 504 nm spectrophotometrically. Oxidation reactions were carried out in 96-well CoStar plates using 10–30 μM dye stock solution with 200 μM hydrogen peroxide (H_2O_2) and different concentrations of L-FABP.

Isolation of lipoproteins

Plasma fractions of <1.21 densities were separated from fresh human plasma by ultracentrifugation in the presence of 1 mM EDTA. After dialysis, plasma lipoproteins were applied on a lysine-Sepharose 4B affinity chromatography column. Unbound lipoproteins were used to prepare Lp(a)-free LDL (density 1.019–1.063) using ultracentrifugation. Lipoproteins were stored in sealed tubes filled with nitrogen and kept in the dark at 4°C to prevent oxidization during storage. Protein concentrations of LDL were measured by a BCA protein kit (Fisher Scientific).

Lipid peroxidation induced by AAPH or AMVN

Lipoprotein peroxidation was induced by two oxygen-derived free radical generators: a hydrophilic radical generator, AAPH, and a lipophilic radical generator, AMVN. All the free radical generators were prepared fresh and preincubated with LDL (1 mg cholesterol/ml) for 90 min at 37°C. AAPH was dissolved in deionized water, whereas AMVN was dissolved in 95% ethanol. The lipid peroxidation product (malonaldehyde, MDA) was determined by the thiobarbituric acid-reactive substance (TBARS) method (24). Briefly, the TBARS assay was used to demonstrate reactive aldehydes from lipid peroxidation, which has been widely accepted as a general marker of free radical production. After incubation for 90 min, the reaction was terminated by addition of 1 ml TBA reagent (0.67%, w/v, TBA in a 15%, w/v, trichloroacetic acid solution and 0.25 N HCl). The reaction mixture was heated to 100°C for 15 min and then cooled on ice. Samples were then centrifuged, resulting in the development of a pink chromogen whose absorbance was measured at 535 nm in a spectrophotometer. Freshly diluted malondialdehyde bis(dimethyl acetal 1,1,3,3-tetramethoxypropane) was used as a reference standard. Thiobarbituric acid reactive substances were expressed as MDA equivalents.

Statistical analysis

Results are expressed as mean ± SD. Appropriate statistical analysis included Student's *t*-test (unpaired) where two groups were compared. Two-way ANOVA was used for multiple comparisons. Statistical significance was considered at $P < 0.05$. The n value refers to the number of experimental assays in each study.

RESULTS

Expression and purification of recombinant glutathione *S*-transferase/L-FABP in *Escherichia coli*

The cDNA fragment encoding the complete rat L-FABP sequence was cloned into the pGEX-6P-2 plasmid downstream of the hybrid glutathione *S*-transferase (GST) tag promoter to allow for the inducible and efficient intracellular expression of rat GST/L-FABP in *E. coli*. Following sonication and removal of the bacterial cell pellet, the soluble GST/L-FABP complex was isolated from bacterial cytosolic proteins. Optimal expression time was evaluated by determining the extent of protein accumulation and degradation using SDS-PAGE analysis of cellular lysates over 1–8 h. Following 6 h of induction, the GST/L-FABP tag reached a peak intracellular concentration of ~80% of total *E. coli* intracellular protein, and 0.1 mM isopropyl-β-D-thio-galactoside was sufficient to induce a maximum level of GST/L-FABP expression.

GST/L-FABP was purified to homogeneity by three successive elution steps using GST 4B beads, which precipitated 85% of the GST/L-FABP. This purification method had the highest protein recovery and optimal elution characteristics for GST/L-FABP separation. Following elution, ~50–60 mg of GST/L-FABP was obtained from a 500 ml culture. Impurities were not present as observed by SDS-PAGE on 15% polyacrylamide gels. Thus, contaminants could be effectively removed from the GST/L-FABP complex by GST 4B beads.

Purified recombinant L-FABP was successfully isolated after incubating the GST/L-FABP complex with PreScission Protease and cleavage buffer. SDS-PAGE results showed that our recombinant L-FABP had the same molecular weight (~14 kDa) as L-FABP isolated from hepatoma cells.

Effect of recombinant L-FABP on DCF fluorescence in vitro

The DCF fluorescence assay was used as a convenient screening method for assessing the extent of the antioxidative potential of our recombinant L-FABP. Since intracellular L-FABP has been reported to play a major role in suppressing oxidative stress (20, 22), a reduction in ROS by L-FABP would be observed in an in vitro DCF oxidation assay. As shown in **Fig. 1**, our recombinant L-FABP inhibited H_2O_2-induced free radical levels as observed by a decrease in DCF fluorescence intensity. Moreover, inhibition of the

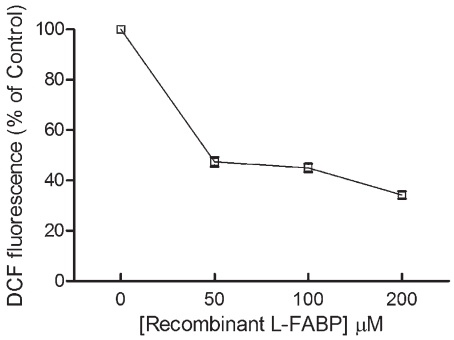

Fig. 1. DCF fluorescence intensity versus recombinant L-FABP concentration. ROS levels were assessed by quantitating the DCF fluorescence intensity at the various concentrations of recombinant L-FABP. The DCFH-DA was deesterified in vitro to give a final concentration of 60 μM stock solution. Reactions were carried out using 10–30 μM activated DCFH stock solution in 96-well plates with 200 μM H_2O_2 and varying concentrations of L-FABP encompassing the lower physiological range. Data are presented as mean ± SD (n = 4). There was a significant difference in DCF fluorescence intensity at the different L-FABP concentrations compared with the control group (0 μM L-FABP); ***$P < 0.001$.

released free radicals was increased with increased L-FABP concentration. Suppression of free radical release was greatest at 200 μM L-FABP, which was observed to be 66 ± 1% of control values ($P < 0.001$). To determine the possibility that L-FABP quenched the DCF fluorescence by binding DCF or by some other unknown mechanism, Rajaraman et al. (22) investigated the quenching potential of L-FABP. They reported that fluorescence was not affected by L-FABP concentration. Thus, results in this study support the notion that the associated decrease in DCF fluorescence was in fact due to L-FABP inactivation of free radicals.

Effect of recombinant L-FABP on lipid peroxidation in the presence of AAPH and AMVN in vitro

To compare the effectiveness of antioxidants in both lipophilic and hydrophilic free radical generating systems, it was necessary to examine the effects of AAPH and AMVN free radical generators in a LDL solution. Levels of the lipid peroxidation product (MDA) were first examined as a function of varying concentrations of AMVN or AAPH (**Fig. 2A**). The lipid-soluble peroxyl radical generator (AMVN) induced greater MDA production in LDL than the water-soluble generator (AAPH). Thus, for subsequent comparison, it was necessary to use AAPH and AMVN concentrations that induced similar amounts of MDA production. The same amount of MDA was produced by 10 mM AMVN and 40 mM AAPH. Therefore, those concentrations were used in all in vitro studies.

Protection by ascorbic acid and α-tocopherol against lipid peroxidation induced by AAPH or AMVN

To compare the difference of antioxidant activity between L-FABP and ascorbic acid or α-tocopherol, LDL was incubated with 40 mM AAPH or 10 mM AMVN in the absence or the presence of different concentrations of ascorbic acid or α-tocopherol (**Fig. 3A**, B). These two antioxidants inhibited the oxidation of LDL in a dose-dependent manner. Using the AAPH generator, 1 mM ascorbic acid was able to reduce MDA production by 60% ($P < 0.001$) (Fig. 3A), whereas no significant protective effect against lipid peroxidation was observed in the 0–40 mM concentration range in the AMVN assay. At a concentration of 5 μM, α-tocopherol reduced >70% of MDA formation (Fig. 3A). The same concentration of α-tocopherol inhibited MDA production by <50% in the AMVN-induced lipid peroxidation assay (Fig. 3B), showing that α-tocopherol has a weaker effect in the inhibition of LDL oxidation by AMVN.

Protection against lipid peroxidation of recombinant L-FABP in AAPH and AMVN

We were interested in knowing whether L-FABP is more effective as a hydrophilic or lipophilic free radical scavenger. Since L-FABP is water soluble, it is thought that most of the antioxidant properties may be directed in the cytosol. However, as a protein it also imparts some lipophilic properties, and as such some of the antioxidant property may be directed at the lipophilic or cell membrane environment. Thus, we investigated the LDL oxidation levels mediated by 40 mM AAPH or 10 mM AMVN in the absence or presence of different L-FABP concentrations using an in vitro system. Figure 2B shows a dose-dependent inhibition in oxidized LDL by 1–20 μM L-FABP on AAPH- and AMVN-induced MDA production. Using AAPH to produce free radicals, a concentration of 1 μM L-FABP was able to reduce MDA formation by 40% ($P < 0.001$), and a 90% ($P < 0.001$) reduction in MDA formation was obtained when the concentration of L-FABP was increased to 20 μM. Figure 3A shows that 10 μM L-FABP inhibited a similar amount of MDA production as 10 mM ascorbic acid but inhibited more MDA production than 10 μM α-tocopherol ($P < 0.01$). At a concentration of 20 μM L-FABP, L-FABP protected against free radical damage much more than either 20 μM α-tocopherol ($P < 0.001$) or 20 mM ascorbic acid ($P < 0.001$).

L-FABP was less potent against MDA production when free radicals were induced by AMVN. Figure 3B shows that

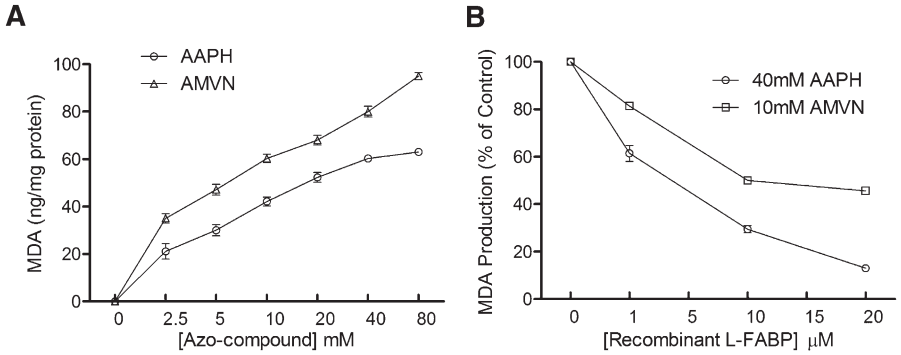

Fig. 2. MDA formation in the presence of various concentrations of AMVN, AAPH, or L-FABP. A: MDA formation at various concentrations of AAPH and AMVN. LDL (1 mg cholesterol/ml) was incubated with different concentrations of AAPH and AMVN at 37°C for 90 min. Effect of 40 mM AAPH and 10 mM AMVN produced the same amount of MDA. B: The effect of recombinant L-FABP on AAPH- and AMVN-induced MDA production on LDL. LDL (1 mg cholesterol/ml) was incubated with 40 mM AAPH or 10 mM AMVN with various concentrations of L-FABP at 37°C for 90 min. Graph shows the dose-dependent manner of recombinant L-FABP in the protection of LDL peroxidation. L-FABP concentration in hepatocytes is ~200–400 μM (34). Values are presented as means ± SD, n = 6, *** $P < 0.001$.

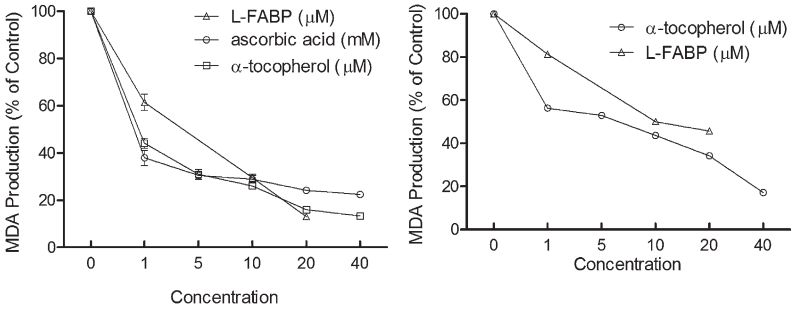

Fig. 3. Comparison of the effect of ascorbic acid, α-tocopherol, and L-FABP on AAPH- and AMVN-induced MDA production on LDL. A: LDL (1 mg cholesterol/ml) was incubated with 40 mM AAPH ± different concentrations of ascorbic acid, α-tocopherol, and L-FABP for 90 min at 37°C. B: LDL (1 mg cholesterol/ml) was incubated with 10 mM AMVN and different concentrations of α-tocopherol and L-FABP for 90 min at 37°C. Values are presented as means ± SD, n = 6, *** $P < 0.001$.

20 μM L-FABP provided greater antioxidant effect against lipid peroxidation induced by AAPH (90%) than that of AMVN (55%). Figure 3B also shows that 10 μM L-FABP inhibited 50% of MDA production and had a similar effect to that of 10 μM α-tocopherol in the AMVN-induced lipophilic free radical generating system. Thus, the antioxidant activity of L-FABP was comparable to α-tocopherol and much greater than ascorbic acid at the same molar concentrations.

Antioxidant effect of L-FABP upon binding of palmitate or α-bromo-palmitate

To understand whether long-chain fatty acid binding to L-FABP influences its antioxidant activity, LDL was incubated with 40 mM AAPH or 10 mM AMVN in the absence or presence of 10 μM L-FABP, which was preincubated with 30 μM α-bromo-palmitate (α-bromo-palmitate is not metabolized) or 30 μM palmitate (reversible binding). In the AAPH-induced lipid peroxidation system, 10 μM L-FABP was able to significantly reduce MDA production by 70 ± 2% ($P < 0.001$), while α-bromo-palmitate and palmitate partially blocked the L-FABP antioxidative activity by 29 ± 2% and 19 ± 1%, respectively (see **Fig. 4**; compared with L-FABP no binding; $P < 0.001$). Figure 4 also shows that in the AMVN-induced lipid peroxidation system, 10 μM L-FABP was able to reduce MDA production by 50 ± 1%, while α-bromo-palmitate and palmitate blocked L-FABP antioxidative activity by 43 ± 1% and 11 ± 1%, respectively (compared with L-FABP no binding; $P < 0.001$). These results indicated that by blocking the L-FABP binding cavity some of the L-FABP antioxidant activity was eliminated.

Identification of L-FABP amino acids involved in the antioxidant effect by MALDI QqTOF MS

Identification of the modified recombinant L-FABP. Recombinant L-FABP was analyzed following separation using chromatography by MALDI QqTOF MS. The amino acid sequence of our recombinant rat L-FABP (**Table 1**) was identical with that of L-FABP isolated from rat liver (25). MALDI-TOF analysis showed presence of a major mass peak at *m/z* of 15,275.9 (**Fig. 5A**). Total measured mass (15,274.9 Da) of L-FABP was greater than that predicted based on the amino acid sequence (14,272.450 Da). The increased mass was attributed to additional amino acids on the N-terminal end and *S*-glutathionylation of the cysteine group, which was observed following peptide mass fingerprinting of L-FABP by in-solution digestion with endoproteinase Glu-C and trypsin and analyzed by MALDI-TOF MS. MS/MS measurements of the N-terminal peptide at *m/z* 2,242.085 showed that the amino acid sequence GPLGSLAT was present in front of the protein translation start codon methionine. Presence of the GPLGSLAT sequence (with an increased mass of 696.382 Da) observed at the N terminus was derived from the GST infusion linker excised by PreScission protease. This peptide fragment has been reported to prevent protein degradation (26). Also, sequence of the peptide (58–80) at *m/z* 2941.316 was confirmed as VIHNEFTLGEE**C**ELETMTGEKVK after trypsin digestion in MS/MS spectrum. This segment included the incorporation of a glutathione onto Cys[69] yielding an additional mass of 305 Da. This finding is consistent with the recombinant GST/L-FABP eluted by reduced glutathione. Thus, the additional mass of 696.382 Da together with the mass of the *S*-glutathionylation product (305.068 Da) yielded our total L-FABP mass of 15,273.900 Da. A more complete MALDI MS analysis of the observed peptide sequences of two enzymatic digests by trypsin and endoprotease Glu-C is listed in Table 1.

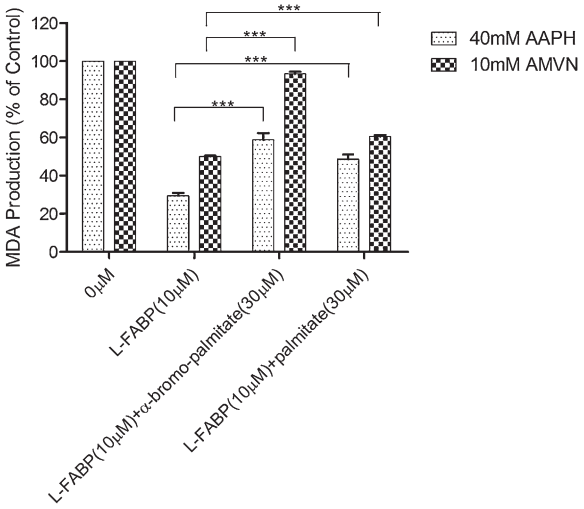

Fig. 4. Comparison of the effect of recombinant L-FABP after binding with palmitate or α-bromo-palmitate on AAPH- or AMVN-induced MDA production on LDL. LDL (1 mg cholesterol/ml) was incubated with 40 mM AAPH or 10 mM AMVN for 90 min at 37°C in the presence or absence of L-FABP (10 μM), palmitate (30 μM), or α-bromo-palmitate (30 μM). Values represent mean ± SD, n = 6, ***$P < 0.001$.

TABLE 1. L-FABP protein sequence identification by MALDI QqTOF mass spectrometry

Enzyme	Observed Peptide	Peptide Sequence	Meas. Value *m/z*	Calc. Mass MH+
Trypsin	Tag-1-6	**GPLGSLAT**MNFSGK	1,379.695	1,379.699
	7-20	YQVQSQENFEPFMK	1,774.804	1,774.811
	21-31	AMGLPEDLIQK	1,214.648	1,214.645
	21-33	AMGLPEDLIQKGK	1,399.767	1,399.761
	21-36	AMGLPEDLIQKGKDIK	1,755.972	1,755.967
	37-46	GVSEIVHEGK	1,054.549	1,054.553
	37-47	GVSEIVHEGKK	1,182.652	1,182.648
	50-57	LTITYGSK	882.492	882.493
	58-80	VIHNEFTLGEE**C***ELETMTGEKVK	2,941.316	2,941.326
	81-96	AVVKMEGDNKMVTTFK	1,797.919	1,797.924
	97-122	GIKSVTEFNGDTITNTMTLGDIVYKR	2,873.467	2,873.471
	100-121	SVTEFNGDTITNTMTLGDIVYK	2,419.176	2,419.179
	100-122	SVTEFNGDTITNTMTLGDIVYKR	2,575.268	2,575.271
	100-125	SVTEFNGDTITNTMTLGDIVYKRVSK	2,889.469	2,889.466
Glu-C				
	Tag-1-13	**GPLGSLAT**MNFSGKYQVQSQE	2,242.085	2,242.081
	14-26	NFEPFMKAMGLPE	1,510.703	1,510.707
	27-40	DLIQKGKDIKGVSE	1,529.851	1,529.853
	14-40	NFEPFMKAMGLPEDLIQKGKDIKGVSE	3,021.525	3,021.542
	14-44	NFEPFMKAMGLPEDLIQKGKDIKGVSEIVHE	3,499.683	3,499.796
	45-62	GKKVKLTITYGSKVIHNE	2,015.158	2,015.165
	78-86	KVKAVVKME	1,031.623	1,031.628
	87-103	GDNKMVTTFKGIKSVTE	1,854.958	1,854.963
	104-121	FNGDTITNTMTLGDIVYK	2,002.977	2,002.979
	104-127	FNGDTITNTMTLGDIVYKRVSKRI	2,742.473	2,742.461

001 MNFSGKYQVQ SQENFEPFMK AMGLPEDLIQ KGKDIKGVSE IVHEGKKVKL.
051 TITYGSKVIH NEFTLGEECE LETMTGEKVK AVVKMEGDNK MVTTFKGIKS.
101 VTEFNGDTIT NTMTLGDIVY KRVSKRI.

The numbers immediately to the left of the amino acids signify the position of that amino acid. Seven methionines located at the L-FABP sequence positions Met1, Met19, Met22, Met74, Met85, Met91, and Met113. The single cysteine is located at sequence position Cys69. * Cys69 is glutathionylated.

To identify the modification of L-FABP by AAPH or AMVN, 100 μM L-FABP was incubated with 40 mM AAPH or 10 mM AMVN and analyzed following separation using chromatography by MALDI-TOF MS. Analysis showed the major mass peak shift from *m/z* of 15,275.9 (L-FABP, Fig. 5A) to 15,291.0 (L-FABP+AMVN, Fig. 5B) or 15,352.0 (L-FABP+AAPH, Fig. 5C). The mass shift of *m/z* 15,275.9 corresponded to ~80 Da oxidation product induced by AAPH. The mass shift of *m/z* 15,291.0 corresponded to a 16 Da oxidation product induced by AMVN.

Identification of the oxidized methionine residues. To verify the L-FABP oxidative peptides after incubation with AAPH or AMVN, 100 μM L-FABP was incubated with 40 mM AAPH or 10 mM AMVN, and the modified peptide mass fingerprinting of the samples was carried out by in-solution digestion with endoproteinase Glu-C and analyzed by MALDI-TOF MS (L-FABP, **Fig. 6A**; L-FABP+AMVN, Fig. 6B; L-FABP+AAPH, Fig. 6C). The methionine-containing peptides in the Glu-C digestion of FABPs are shown in **Table 2**. In the MALDI MS spectrum of AAPH-modified L-FABP (Fig. 6C), the observed product 1-13+OX (*m/z* 2258.080), 14-26+OX/2OX (*m/z* 1526.705, 1542.706), 14-40+OX/2OX (*m/z* 3037.522, 3053.555), 87-103+OX (*m/z* 1870.946), and 104-127+OX (*m/z* 2758.464) (OX = oxidized) correspond to five oxidized methionine (Met^{1}, Met^{19}, Met^{22}, Met^{91}, and Met^{113}) containing fragments, each provide evidence for oxidant modification of methionine by AAPH-induced free radicals. In the MALDI MS spectrum of AMVN-modified L-FABP (Fig. 6B), the ob-

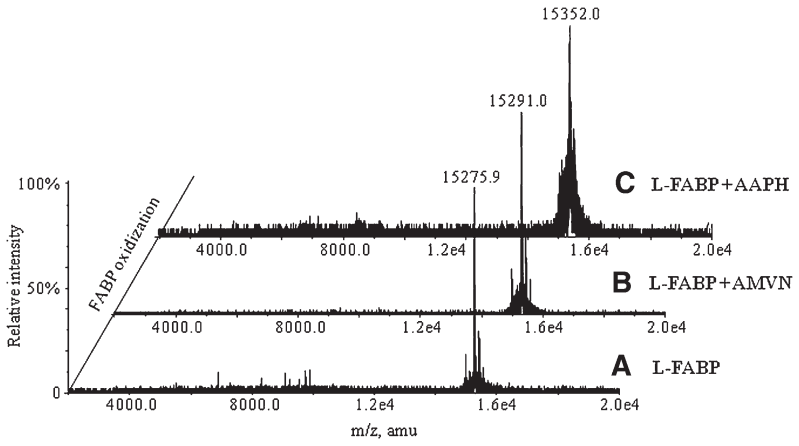

Fig. 5. MALDI QqTOF MS spectra of recombinant L-FABP (A) and L-FABP incubated with 10 mM AMVN (B) or 40 mM AAPH (C). Samples were separated from any impurities by column chromatography, desalted, and subjected to MALDI QqTOF MS analysis. A: The high intensity peak at *m/z* 15,275.9 corresponds to the molecular mass of the purified recombinant L-FABP. B: The high intensity peak at *m/z* 15,291.0 corresponds to the molecular mass of the recombinant L-FABP incubated with 10 mM AMVN. C: The high intensity peak at *m/z* 15,352.0 corresponds to the molecular mass of the recombinant L-FABP incubated with 40 mM AAPH.

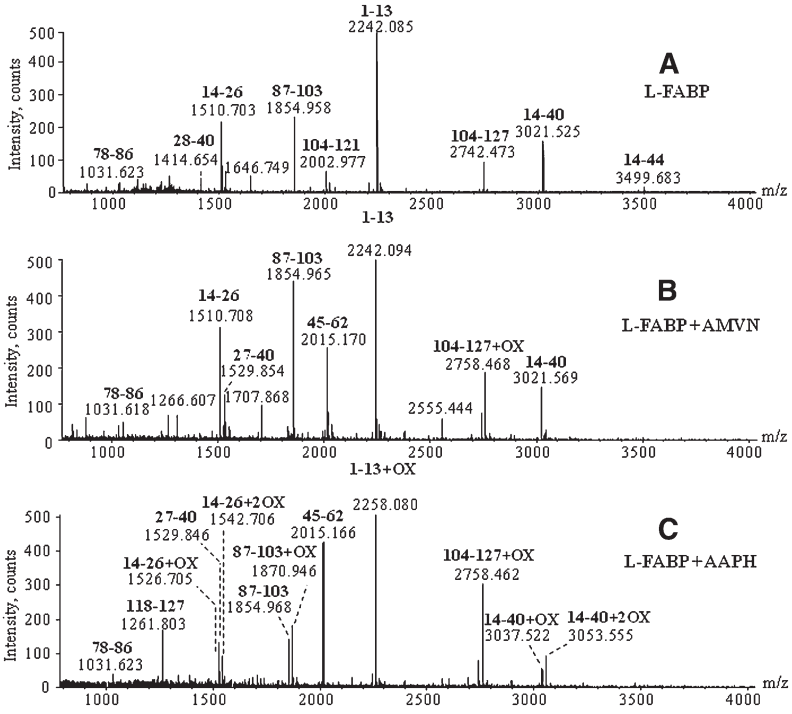

Fig. 6. MALDI QqTOF MS spectra of the Glu-C digest of recombinant L-FABP containing peptide. A: purified recombinant L-FABP. B: Recombinant L-FABP incubated with 10 mM AMVN. C: Recombinant L-FABP incubated with 40 mM AAPH.

served product 104-127+OX (*m/z* 2758.468) (OX = oxidized) corresponded to one oxidized methionine (Met^{113}) containing fragment, which provided evidence for oxidant modification of methionine by AMVN-induced free radicals.

DISCUSSION

Attack by free radicals on lipophilic structures, such as cell membranes or intracellular membranes, may result in severe forms of cell damage and/or ultimately cell death. Lipid peroxidation products are especially of importance since they are highly reactive and able to form adducts with many cellular lipophilic macromolecules, including cell membrane constituents, intracellular proteins, and nucleic acids (27). These adducts modify the structure and function of these cellular components and are involved in the pathogenesis of various degenerative diseases, including heart disease (28), diabetes (29), inflammation (30), and neurodegenerative disorders (31). Although cells contain specific endogenous antioxidant enzymes, such as superoxide dismutase, catalase, glutathione peroxidase, and compounds such as β-carotene and tocopherols, levels of these antioxidants may be too low to combat the high concentrations of released free radicals especially during periods of oxidative stress. Moreover, many of these antioxidants direct their activity toward the aqueous milieu. However, α-tocopherol is a fat-soluble vitamin that may have some of its activity directed toward lipophilic structures (32).

Recent work has shown that in addition to being the intracellular counterpart to extracellular albumin, L-FABP

TABLE 2. MALDI MS analyses of the methionine-containing peptides in the Glu-C digests of FABPs

Calc. [MH]+	Peptide Fragment	Peptide Sequence	Oxidized Residue	Observed Relative Intensity Ratios between the Unmodified Peptide and Its Oxidized Peptide Counterparts [a] L-FABP	L-FABP- 40 mMAAPH	L-FABP- 10 mMAMVN
1,031.6281,047.623	78-86	KVKAVVKME	Met^{85}	100%	100%	100%
	78-86 + OX			0%	–[b]	–
1,510.707	14-26	NFEPFMKAMGLPE	Met^{19}	91%	10%	91%
1,526.702	14-26+OX[c]		Met^{22}	9%	41%	9%
1,542.697	14-26+2OX			0%	49%	–
1,854.963	87-103	GDNKMVTTFKGIKSVTE	Met^{91}	100%	44%	100%
1,870.958	87-103+OX			0%	56%	–
2,242.084	1-13	GPLGSLATMNFSGKYQVQSQE	Met^{1}	94%	9%	88%
2,258.080	1-13+OX			6%	91%	12%
2,742.461	104-127	FNGDTITNTMTLGDIVYKRVSKRI	Met^{113}	91%	21%	17%
2,758.456	104-127+OX			9%	79%	83%

[a] Percentage of the observed peptide peaks: the peak intensity/Σ (the unmodified peptide intensity + its oxidized peptide intensity).
[b] Denotes the unobserved peak.
[c] Met^{22} was the first oxidization site in this peptide as confirmed by MS/MS measurements.

possesses strong antioxidant properties. In fact, when clofibrate was used to increase L-FABP levels in animals subjected to bile-duct ligation, clofibrate-treated animals were shown to be associated with reduced levels of hepatic lipid peroxidation products and improved hepatic function (21). Clofibrate-treated animals were also associated with lower levels of mortality (G. Wang, H. Shen, G. Rajaraman, M.S. Roberts, Y. Gong, P. Jiang, F.Burczynski, unpublished observations). The authors speculated that L-FABP functions as an antioxidant during periods of cellular oxidative stress. Moreover, in a cell transfection model, hepatocytes containing L-FABP were associated with much lower ROS levels than those devoid of L-FABP (20). In both models, levels of the endogenous antioxidants were unaffected by the treatment regime. The mechanism whereby L-FABP inactivated ROS, however, was not understood. Understanding the protein's antioxidant mechanism of action required in vitro studies and large amounts of rat L-FABP.

In this study, recombinant L-FABP was successfully expressed in *E. coli* using a simple purification system. The system made use of a GST affinity tag that allowed for a more efficient purification of the recombinant protein in *E. coli* (33). The GST tag contained a site whereby ProScission protease could cleave the GST tag allowing for greater sequence specificity in generating the target protein. A small sequence chain remained on the target protein at the N terminus after the removal of the GST tag. This prevented protein degradation and maintained immunogenicity of the protein (26). After removal of the GST tag from the soluble GST/L-FABP fusion, the resulting L-FABP covered a full-length amino acid sequence of rat L-FABP (25).

Purified L-FABP showed high biological activity with respect to its antioxidant activity. Initial studies using H_2O_2 as a nonspecific free radical generator showed that our recombinant protein at 200 μM inactivated ~66 ± 2% of the released free radicals. Since L-FABP makes up ~2% of total cellular protein in hepatocytes or ~200–400 μM (34), this concentration of L-FABP supplies a significant amount of antioxidant activity within hepatocytes. Following clofibrate treatment, the concentration of L-FABP could rise to 2- to 3-fold (35), which would have an even greater impact on intracellular free radical levels and further contribute a significant amount of free radical scavenging activity. It is, therefore, not surprising that L-FABP protected the liver during periods of oxidative stress as was associated with cholestatic liver disease (21), hepatic steatosis (10), or alcohol-induced liver injury (36).

Free radicals such as $O^{\cdot}_2$ and $OH^{\cdot}$ were initially thought to penetrate lipid bilayers with ease (37). However, more recent evidence suggested that superoxides do not penetrate deeply into lipid bilayers but rather react at the surface or just below the surface of membranes (38). AMVN and AAPH are azo initiators that produce a slow and steady source of free radicals by known chemical decomposition mechanisms. AAPH is a water-soluble azo compound. Decomposition produces molecular nitrogen and two carbon radicals. The carbon radicals may combine to produce stable products or react with molecular oxygen to generate hydrophilic peroxyl radicals (39). In the presence of LDL, AAPH released free radicals oxidize the aqueous (outer) environment of LDL (40). AMVN is a synthetic azo compound that dissociates spontaneously to form carbon-centered free radicals. Generation of carbon-centered radicals is directed at the lipophilic environment of membranes, where its activity is sufficient to cause membrane phospholipid peroxidation (41).

Using the free radical generators AAPH and AMVN together with use of the positive controls ascorbic acid (hydrophilic antioxidant) and α-tocopherol (lipophilic antioxidant), we assessed the effectiveness of L-FABP as an antioxidant. Both α-tocopherol and ascorbic acid were effective in protecting LDL from free radicals generated by AAPH. Using AMVN, however, ascorbic acid had no effect on inactivating free radicals, while not surprisingly α-tocopherol was very effective. L-FABP was effective in inactivating free radicals released by both AAPH and AMVN. L-FABP is known to coat the surface of anionic phospholipid membranes (42) and can prevent propagation of phospholipid oxidation reactions by reacting with the ROS in this environment. Where this becomes of importance is in the protection of cellular membranes during episodes of oxidative stress whereby lipophilic antioxidants have been shown to be effective in suppressing the progression of fatty liver disease (43), coronary heart disease (44), and aging (45).

MALDI-TOF analysis was used to identify the mechanism of L-FABP's antioxidant activity. Amino acid sequence identification showed that our recombinant protein contained one cysteine and seven methionines, which was identical to the sequence reported by others (25, 46). Methionine residues in proteins are known to be oxidized to methionine sulfoxides [Met(O)] by ROS and can be reduced back to the original form by methionine sulfoxide reductase (47). Sequence identification showed that in the AAPH hydrophilic system, five of the seven methionine amino acids were oxidized. These included Met^{19}, Met^{22}, Met^{91}, Met^{1}, and Met^{113}. Of these five amino acids, Met^{1} was almost totally oxidized, followed by Met^{113}, Met^{91}, Met^{22}, and Met^{19}. Met^{85} and Met^{74} were unavailable for reaction with free radicals. This is likely due to the positioning of these amino acids within the protein itself. Met^{74} is located at the L-FABP binding cavity side chain located on the βEβF hairpin turn. This is an area of low solvent accessibility making it difficult to be accessible to free radicals (6). Therefore, it is not surprising to observe that Met^{74} was not easily oxidized in either the AAPH or AMVN free radical systems. Binding of free radicals to one amino acid also may cause a slight change in protein structure through ring opening (48), which could make other amino acids available or unavailable for reaction. Using the lipophilic-free radical generator AMVN, three of the seven methionines in our L-FABP were available for reaction. While Met^{74} and Met^{85} were unreactive in both systems, Met^{91} was unreactive in the lipophilic system. Met^{113} was the only methionine residue with the highest degree of availability to free radicals (83%) in the AMVN system. Thus, MALDI-TOF

MS analysis showed that, indeed, several of the methionine groups in L-FABP do react with free radicals. Similarly, the single cysteine group (Cys^{69}) of L-FABP in the presence of free radicals can form a sulfonic acid intermediate (Cys-SOH) that is subsequently reduced back by forming a disulfide bond through the action of thioredoxin (49). Reactivity of various amino acids was investigated by Xu and Chance (48). They showed that cysteine and methionine were the most reactive of all the amino acids. The cysteine group in our recombinant L-FABP was unavailable for reaction with free radicals because it was *S*-glutathionylated during the GST/L-FABP elution process by reduced glutathione. However, cysteine is well known to be highly effective in scavenging free radicals (50) and thus also makes it a likely candidate in L-FABP's antioxidant activity.

To understand the contribution of L-FABP's binding pocket to its antioxidant activity in both the hydrophilic and lipophilic free radical generating systems, we incubated L-FABP with palmitate or α-bromo-palmitate. Palmitate binding to L-FABP is a reversible process with distinct association and dissociation rate constants (51). α-Bromo-palmitate does not undergo esterification to form triglycerides; its lack of metabolism allows it to accumulate in the cytoplasm making it relatively more effective at binding to L-FABP compared with palmitate (52). Binding of palmitate to L-FABP decreased L-FABP's ability to inactivate free radicals, i.e., binding of long-chain fatty acids to L-FABP increased the amount of free radicals within the hydrophilic and lipophilic environments. The amount of ROS generated by AMVN was slightly higher than that generated by AAPH, suggesting that when palmitate is bound to the protein some methionine group(s) may be inaccessible for reaction with free radicals. This is especially evident in the lipophilic environment. Binding of α-bromo-palmitate to L-FABP resulted in a much more dramatic increase in ROS levels using the AMVN generator. While both systems resulted in higher ROS levels, these levels were much higher in the lipophilic system. Met^{113} is known to be located in the binding cavity of L-FABP (6). Since α-bromo-palmitate is not metabolized, it would be expected to bind to a larger extent than palmitate and block the accessibility of ROS to this amino acid. Similarly, binding of polyunsaturated long-chain fatty acids possessing binding constants much higher than that of palmitate would be expected to have higher binding occupancy rates. In such cases, Met^{113} would not be available for interaction with ROS. The methionine group within the L-FABP binding cavity is therefore of more importance when scavenging free radicals within a lipophilic environment. Met^{1} and Met^{22} are the only other two methionine groups that have the ability to react with ROS but to a much lesser extent than Met^{113}. This is likely the reason why binding of α-bromo-palmitate to L-FABP in the AMVN system did not totally abolish the antioxidant effect of L-FABP. One could speculate that as L-FABP comes in close proximity to the membrane surface; the protein orientates itself such that the ligand binding pocket face is open to the membrane. This could occur by electrostatic interactions between the cell surface and protein. Such interactions have been shown to occur for heart-FABP and membranes (53). In this manner, L-FABP could interact with ROS at lipophilic interfaces. The fact that only 10% of the released free radicals were scavenged by L-FABP in the presence of α-bromo-palmitate indicated that Met^{113} in L-FABP binding cavity is likely the key amino acid that is mostly responsible for L-FABP antioxidant activity in AMVN-induced lipid peroxidation.

In summary, the GST fusion system provided a simple and convenient way to produce large quantities of recombinant L-FABP. The TBARS assay showed that L-FABP protected LDL from oxidation with a similar potency to α-tocopherol but much greater potency than ascorbic acid. MALDI-TOF MS analysis showed that the methionine groups of L-FABP were responsible for the majority of its antioxidant activity in both lipophilic and hydrophilic systems. Met^{113} located in the L-FABP binding cavity was shown to be the most important amino acid for reacting with ROS in the lipophilic free radical generating system. These results demonstrate that rat L-FABP can act as a potent cellular antioxidant.

REFERENCES

1. Glatz, J. F., and G. J. van der Vusse. 1996. Cellular fatty acid-binding proteins: their function and physiological significance. *Prog. Lipid Res.* **35:** 243–282.
2. Ockner, R. K., J. A. Manning, R. B. Poppenhausen, and W. K. Ho. 1972. A binding protein for fatty acids in cytosol of intestinal mucosa, liver, myocardium, and other tissues. *Science.* **177:** 56–58.
3. Schachtrup, C., T. E. Scholzen, V. Grau, T. A. Luger, C. Sorg, F. Spener, and C. Kerkhoff. 2004. L-FABP is exclusively expressed in alveolar macrophages within the myeloid lineage: evidence for a PPARalpha-independent expression. *Int. J. Biochem. Cell Biol.* **36:** 2042–2053.
4. Yamamoto, T., E. Noiri, Y. Ono, K. Doi, K. Negishi, A. Kamijo, K. Kimura, T. Fujita, T. Kinukawa, H. Taniguchi, et al. 2007. Renal L-type fatty acid–binding protein in acute ischemic injury. *J. Am. Soc. Nephrol.* **18:** 2894–2902.
5. Neeli, I., S. A. Siddiqi, S. Siddiqi, J. Mahan, W. S. Lagakos, B. Binas, T. Gheyi, J. Storch, and C. M. Mansbach 2nd. 2007. Liver fatty acid-binding protein initiates budding of pre-chylomicron transport vesicles from intestinal endoplasmic reticulum. *J. Biol. Chem.* **282:** 17974–17984.
6. Thompson, J., N. Winter, D. Terwey, J. Bratt, and L. Banaszak. 1997. The crystal structure of the liver fatty acid-binding protein. A complex with two bound oleates. *J. Biol. Chem.* **272:** 7140–7150.
7. Norris, A. W., and A. A. Spector. 2002. Very long chain n-3 and n-6 polyunsaturated fatty acids bind strongly to liver fatty acid-binding protein. *J. Lipid Res.* **43:** 646–653.
8. Martin, G. G., B. P. Atshaves, A. L. McIntosh, J. T. Mackie, A. B. Kier, and F. Schroeder. 2008. Liver fatty acid-binding protein gene-ablated female mice exhibit increased age-dependent obesity. *J. Nutr.* **138:** 1859–1865.
9. Thumser, A. E., and J. Storch. 2000. Liver and intestinal fatty acid-binding proteins obtain fatty acids from phospholipid membranes by different mechanisms. *J. Lipid Res.* **41:** 647–656.
10. Martin, G. G., B. P. Atshaves, A. L. McIntosh, J. T. Mackie, A. B. Kier, and F. Schroeder. 2005. Liver fatty-acid-binding protein (L-FABP) gene ablation alters liver bile acid metabolism in male mice. *Biochem. J.* **391:** 549–560.
11. Raza, H., J. R. Pongubala, and S. Sorof. 1989. Specific high affinity binding of lipoxygenase metabolites of arachidonic acid by liver fatty acid binding protein. *Biochem. Biophys. Res. Commun.* **161:** 448–455.
12. Jefferson, J. R., J. P. Slotte, G. Nemecz, A. Pastuszyn, T. J. Scallen, and F. Schroeder. 1991. Intracellular sterol distribution in transfected mouse L-cell fibroblasts expressing rat liver fatty acid-binding protein. *J. Biol. Chem.* **266:** 5486–5496.
13. Hsu, K. T., and J. Storch. 1996. Fatty acid transfer from liver and intestinal fatty acid-binding proteins to membranes occurs by different mechanisms. *J. Biol. Chem.* **271:** 13317–13323.

14. Storch, J., and A. E. Thumser. 2000. The fatty acid transport function of fatty acid-binding proteins. *Biochim. Biophys. Acta.* **1486:** 28–44.
15. Schroeder, F., A. D. Petrescu, H. Huang, B. P. Atshaves, A. L. McIntosh, G. G. Martin, H. A. Hostetler, A. Vespa, D. Landrock, K. K. Landrock, et al. 2008. Role of fatty acid binding proteins and long chain fatty acids in modulating nuclear receptors and gene transcription. *Lipids.* **43:** 1–17.
16. Hostetler, H. A., A. B. Kier, and F. Schroeder. 2006. Very-long-chain and branched-chain fatty acyl-CoAs are high affinity ligands for the peroxisome proliferator-activated receptor alpha (PPARalpha). *Biochemistry.* **45:** 7669–7681.
17. Gossett, R. E., A. A. Frolov, J. B. Roths, W. D. Behnke, A. B. Kier, and F. Schroeder. 1996. Acyl-CoA binding proteins: multiplicity and function. *Lipids.* **31:** 895–918.
18. Binas, B., and E. Erol. 2007. FABPs as determinants of myocellular and hepatic fuel metabolism. *Mol. Cell. Biochem.* **299:** 75–84.
19. Ek, B. A., D. P. Cistola, J. A. Hamilton, T. L. Kaduce, and A. A. Spector. 1997. Fatty acid binding proteins reduce 15-lipoxygenase-induced oxygenation of linoleic acid and arachidonic acid. *Biochim. Biophys. Acta.* **1346:** 75–85.
20. Wang, G., Y. Gong, J. Anderson, D. Sun, G. Minuk, M. S. Roberts, and F. J. Burczynski. 2005. Antioxidative function of L-FABP in L-FABP stably transfected Chang liver cells. *Hepatology.* **42:** 871–879.
21. Wang, G., H. Shen, G. Rajaraman, M. S. Roberts, Y. Gong, P. Jiang, and F. Burczynski. 2007. Expression and antioxidant function of liver fatty acid binding protein in normal and bile-duct ligated rats. *Eur. J. Pharmacol.* **560:** 61–68.
22. Rajaraman, G., G. Q. Wang, J. Yan, P. Jiang, Y. Gong, and F. J. Burczynski. 2007. Role of cytosolic liver fatty acid binding protein in hepatocellular oxidative stress: effect of dexamethasone and clofibrate treatment. *Mol. Cell. Biochem.* **295:** 27–34.
23. Wang, G., Q. M. Chen, G. Y. Minuk, Y. Gong, and F. J. Burczynski. 2004. Enhanced expression of cytosolic fatty acid binding protein and fatty acid uptake during liver regeneration in rats. *Mol. Cell. Biochem.* **262:** 41–49.
24. Buege, J. A., and S. D. Aust. 1978. Microsomal lipid peroxidation. *Methods Enzymol.* **52:** 302–310.
25. She, Y. M., G. Q. Wang, A. Loboda, W. Ens, K. G. Standing, and F. J. Burczynski. 2002. Sequencing of rat liver cytosolic proteins by matrix-assisted laser desorption ionization-quadrupole time-of-flight mass spectrometry following electrophoretic separation and extraction. *Anal. Biochem.* **310:** 137–147.
26. Carr, S., J. Miller, S. E. Leary, A. M. Bennett, A. Ho, and E. D. Williamson. 1999. Expression of a recombinant form of the V antigen of *Yersinia pestis*, using three different expression systems. *Vaccine.* **18:** 153–159.
27. Moller, P., and H. Wallin. 1998. Adduct formation, mutagenesis and nucleotide excision repair of DNA damage produced by reactive oxygen species and lipid peroxidation product. *Mutat. Res.* **410:** 271–290.
28. Savchenkova, A. P., L. B. Dudnik, I. L. Pogoretskaya, N. P. Solov'eva, M. A. Pokrovskaya, A. V. Aseichev, S. V. Drinitsyna, O. A. Azizova, and Y. M. Lopukhin. 2003. Effects of fibrinogen on lipid peroxidation in patients with coronary heart disease and in vitro. *Bull. Exp. Biol. Med.* **135:** 29–33.
29. Stadler, K., M. G. Bonini, S. Dallas, J. Jiang, R. Radi, R. P. Mason, and M. B. Kadiiska. 2008. Involvement of inducible nitric oxide synthase in hydroxyl radical-mediated lipid peroxidation in streptozotocin-induced diabetes. *Free Radic Biol Med.* **45:** 866–874.
30. Pang, B., X. Zhou, H. Yu, M. Dong, K. Taghizadeh, J. S. Wishnok, S. R. Tannenbaum, and P. C. Dedon. 2007. Lipid peroxidation dominates the chemistry of DNA adduct formation in a mouse model of inflammation. *Carcinogenesis.* **28:** 1807–1813.
31. Hall, E. D. 1992. Novel inhibitors of iron-dependent lipid peroxidation for neurodegenerative disorders. *Ann. Neurol.* **32(Suppl):** S137–S142.
32. Massey, J. B., H. S. She, and H. J. Pownall. 1982. Interaction of vitamin E with saturated phospholipid bilayers. *Biochem. Biophys. Res. Commun.* **106:** 842–847.
33. Smith, D. B., and K. S. Johnson. 1988. Single-step purification of polypeptides expressed in *Escherichia coli* as fusions with glutathione S-transferase. *Gene.* **67:** 31–40.
34. Burnett, D. A., N. Lysenko, J. A. Manning, and R. K. Ockner. 1979. Utilization of long chain fatty acids by rat liver: studies of the role of fatty acid binding protein. *Gastroenterology.* **77:** 241–249.
35. Bass, N. M., J. A. Manning, R. K. Ockner, J. I. Gordon, S. Seetharam, and D. H. Alpers. 1985. Regulation of the biosynthesis of two distinct fatty acid-binding proteins in rat liver and intestine. Influences of sex difference and of clofibrate. *J. Biol. Chem.* **260:** 1432–1436.
36. Gyamfi, M. A., I. Damjanov, S. French, and Y. J. Wan. 2008. The pathogenesis of ethanol versus methionine and choline deficient diet-induced liver injury. *Biochem. Pharmacol.* **75:** 981–995.
37. Wagner, B. A., G. R. Buettner, L. W. Oberley, C. J. Darby, and C. P. Burns. 2000. Myeloperoxidase is involved in H2O2-induced apoptosis of HL-60 human leukemia cells. *J. Biol. Chem.* **275:** 22461–22469.
38. Gamliel, A., M. Afri, and A. A. Frimer. 2008. Determining radical penetration of lipid bilayers with new lipophilic spin traps. *Free Radic. Biol. Med.* **44:** 1394–1405.
39. Culbertson, S. M., and N. A. Porter. 2000. Design of unsymmetrical azo initiators to increase radical generation efficiency in low-density lipoproteins. *Free Radic. Res.* **33:** 705–718.
40. Scanu, A. M., and C. Wisdom. 1972. Serum lipoproteins structure and function. *Annu. Rev. Biochem.* **41:** 703–730.
41. Niki, E. 1990. Free radical initiators as source of water- or lipid-soluble peroxyl radicals. *Methods Enzymol.* **186:** 100–108.
42. Davies, J. K., A. E. Thumser, and D. C. Wilton. 1999. Binding of recombinant rat liver fatty acid-binding protein to small anionic phospholipid vesicles results in ligand release: a model for interfacial binding and fatty acid targeting. *Biochemistry.* **38:** 16932–16940.
43. Botella-Carretero, J. I., J. A. Balsa, C. Vazquez, R. Peromingo, M. Diaz-Enriquez, and H. F. Escobar-Morreale. 2008. Retinol and alpha-Tocopherol in Morbid Obesity and Nonalcoholic Fatty Liver Disease. *Obes Surg.* In press.
44. Tornwall, M. E., J. Virtamo, P. A. Korhonen, M. J. Virtanen, P. R. Taylor, D. Albanes, and J. K. Huttunen. 2004. Effect of alpha-tocopherol and beta-carotene supplementation on coronary heart disease during the 6-year post-trial follow-up in the ATBC study. *Eur. Heart J.* **25:** 1171–1178.
45. Guarnieri, C., E. Giordano, C. Muscari, L. Grossi, and C. M. Caldarera. 1996. Alpha-tocopherol pretreatment improves endothelium-dependent vasodilation in aortic strips of young and aging rats exposed to oxidative stress. *Mol. Cell. Biochem.* **157:** 223–228.
46. Murphy, E. J., R. D. Edmondson, D. H. Russell, S. Colles, and F. Schroeder. 1999. Isolation and characterization of two distinct forms of liver fatty acid binding protein from the rat. *Biochim. Biophys. Acta.* **1436:** 413–425.
47. Brot, N., and H. Weissbach. 1983. Biochemistry and physiological role of methionine sulfoxide residues in proteins. *Arch. Biochem. Biophys.* **223:** 271–281.
48. Xu, G., and M. R. Chance. 2005. Radiolytic modification and reactivity of amino acid residues serving as structural probes for protein footprinting. *Anal. Chem.* **77:** 4549–4555.
49. Pan, J. L., and J. C. Bardwell. 2006. The origami of thioredoxin-like folds. *Protein Sci.* **15:** 2217–2227.
50. Badaloo, A., M. Reid, T. Forrester, W. C. Heird, and F. Jahoor. 2002. Cysteine supplementation improves the erythrocyte glutathione synthesis rate in children with severe edematous malnutrition. *Am. J. Clin. Nutr.* **76:** 646–652.
51. Hung, D. Y., F. J. Burczynski, P. Chang, A. Lewis, P. P. Masci, G. A. Siebert, Y. G. Anissimov, and M. S. Roberts. 2003. Fatty acid binding protein is a major determinant of hepatic pharmacokinetics of palmitate and its metabolites. *Am. J. Physiol. Gastrointest. Liver Physiol.* **284:** G423–G433.
52. Luxon, B. A. 1996. Inhibition of binding to fatty acid binding protein reduces the intracellular transport of fatty acids. *Am. J. Physiol.* **271:** G113–G120.
53. Herr, F. M., J. Aronson, and J. Storch. 1996. Role of portal region lysine residues in electrostatic interactions between heart fatty acid binding protein and phospholipid membranes. *Biochemistry.* **35:** 1296–1303.